Available online at www.sciencedirect.com
SCIENCE DIRECT®
Biochemical and Biophysical Research Communications 307 (2003) 198–205
BBRC
www.elsevier.com/locate/ybbrc

A peptide mimetic of an anti-CD4 monoclonal antibody by rational design

Florence Casset,[a] Florence Roux,[a] Patrick Mouchet,[a] Cedric Bes,[b] Thierry Chardes,[c] Claude Granier,[b] Jean-Claude Mani,[b] Martine Pugnière,[b] Daniel Laune,[b] Bernard Pau,[b] Michel Kaczorek,[a] Roger Lahana,[a] and Anthony Rees[a,*]

[a] *Synt:em, Parc Scientifique Georges Besse, FR-30035 Nîmes Cédex 1, France*
[b] *Centre de Pharmacologie et Biotechnologie pour la Santé, CNRS UMR 5094, Faculté de Pharmacie, 15 Avenue Charles Flahault, 34093 Montpellier Cedex 5, France*
[c] *Laboratoire de Pathologie Comparée, INRA-cNRS UMR 5087, 30380 Saint Christol les Alès, France*

Received 20 May 2003

This article is dedicated to the memory of Jean-Claude Mani, who passed away before this work was completed.

Abstract

The development of rational methods to design 'continuous' sequence mimetics of discontinuous regions of protein sequence has, to now, been only marginally successful. This has been largely due to the difficulty of constraining the recognition elements of a mimetic structure to the relative conformational and spatial orientations present in the parent molecule. Using peptide mapping to determine 'active' antigen recognition residues, molecular modeling, and a molecular dynamics trajectory analysis, we have developed a peptide mimic of an anti-CD4 antibody, containing antigen contact residues from multiple CDRs. The design described is a 27-residue peptide formed by juxtaposition of residues from 5 CDR regions. It displays an affinity for the antigen (CD4) of 0.9 nM, compared to 2 nM for the parent antibody ST40. Nevertheless, the mimetic shows low biological activity in an anti-retroviral assay.

Keywords: Antibody modeling; Antibody mimetic; Paratope mimetic; Rational design; Anti-CD4 monoclonal antibody; ST40

The design of small oligopeptide, or peptide-like mimics to reproduce the activity of large natural proteins has numerous applications in both therapeutics and diagnostics. Where the activity region of interest is located within a continuous sequence of the protein, methods have been described in which the conformational requirements of such regions can be met by various chemical cross-linking or other synthetic strategies [1,2]. However, where the activity region(s) of a protein consist of discontinuous segments of the polypeptide chain, the problem of mimetic design is particularly acute.

Several approaches have been proposed to mimic the discontinuous binding surface of a protein. Mutter has defined a template approach (TASP, for template-assembled synthetic proteins) where amino acids defined as bioactive are linked to a topological template to mimic the protein activity [3,4]. Others have used small multi-disulfide-containing *mini-proteins* (protease inhibitors and animal toxins) as templates to reproduce the binding surface of a particular protein by mutation of amino acids at the surface of the mini-protein. In one exemplification of this approach, functional sites of CD4 were transferred to a scorpion toxin generating an inhibitor of the HIV-1 gp120-CD4 interaction [5]. Non-peptidyl mimics, in which the spatial arrangement of important amino acid side chains of the parent protein are reproduced, has been also described for protein A [6]. A particularly interesting approach, in which a synthetic cyclic mimic of a discontinuous binding site

* Corresponding author. Fax: +33-4-66-04-86-67.
E-mail address: trees@syntem.com (A. Rees).

0006-291X/03/$ - see front matter © 2003 Elsevier Science (USA). All rights reserved.
doi:10.1016/S0006-291X(03)01131-8

from interleukin-10 was generated using peptide libraries in a multi-step sequence, was described by Reineke et al. [7]. In all, 446 combinations of cyclization were synthesized and tested. The final mimic displayed good activity. Using a similar approach, a peptido-mimetic with a high affinity to rheumatoid arthritis-associated Class II major histocompatibility (MHC) molecules was designed [8]. While novel in their own particular ways, these library based methods are labor and material intensive and lack the design element that will eventually lead to more reproducible and rational mimetic construction.

Mimetics of antibody combining sites represent a particularly interesting target. All antibodies have six CDRs residues all of which are more or less involved in antigen recognition. Thus, the antibody combining site is a predictable, if demanding example of the 'mimetic of a discontinuous surface.' Approaches to date have tended to simplify the problem by targeting the mimetic design to CDR H3, since this CDR is typically at the center of most, if not all, antigen interactions [2]. This has its limitations, however, since clearly other CDRs play an important role in the recognition process. The problem to now has been, how to incorporate residues from different CDRs into a single, synthetically accessible molecular design.

In this paper we described a new approach where a mimetic of the paratope of an antibody was designed in such a way that all the amino acids defined as 'active chemical groups' for the binding activity, and deriving from multiple CDRs, were incorporated into a specific, synthetically accessible, peptide-like construct. The monoclonal antibody (MAb) ST40 was selected to develop this method. This antibody is specific for the CDR3-like loop in domain 1 of the CD4 molecule and, indirectly, inhibits human immunodeficiency virus type 1 (HIV-1) replication.

The starting point for this process is a 3D structure of the target antibody and if possible complexed with its antigen. If no X-ray structure is available (as with ST40), a structure prediction method is required for the antibody and alternative methods like site directed mutation or alanine scanning [9] are required to identify the 'active chemical groups.' In this study, the 3D structure of ST40 was modeled using the research version of the AbM software [10] and the 'active chemical groups' were identified by alanine scanning [11] of synthetic overlapping peptides derived from the ST40 sequence.

Materials and methods

ST40 and alanine scanning

The cloning of MAb ST40 and its alanine scanning is described in [11].

CD4

The human recombinant CD4 used for the kinetic analysis and the biological assays was obtained from RepliGen (USA).

BIAcore analysis

The kinetic parameters, association rate constant (k_a) and dissociation rate constant (k_d), were determined by surface plasmon resonance (SPR) analysis using BIACORE 2000 (Biacore AB, Uppsala, Sweden). k_a and k_d were determined using BIAevaluation 3.0 software (BIAcore AB). The apparent equilibrium constant K_D is the ratio k_d/k_a. All experiments were carried out at 25 °C. The free NH_2 group of the lysine side chain of the mimetic was used to chemically immobilize molecules on a B1 sensor chip (BIAcore AB) following a standard EDC/NHS procedure from BIAcore. The SPR signals for immobilized peptide mimetics were found to be about 280–500 resonance units (RU) after completion of the chip regeneration cycle, which corresponds to 280–500 pg/mm^2. The binding kinetic of CD4 to immobilize the mimetic was determined by injecting several concentrations of CD4 (50–200 nM) in HBS buffer (running buffer) at a flow rate of 30 μl/min. For the selectivity study of the mimetic, the binding kinetics of immobilized mimetic were determined by injecting irrelevant proteins: Troponin C and 2C2 an anti-digoxin mAb, each at 165 nM, in HBS buffer at a flow rate of 30 μl/min. For the competition study, ST40 MAb (660 nM) and CD4 (165 nM) were pre-mixed, then co-injected on the sensor chip.

Protein binding analysis

The peptides were incubated for 10 min at 37 °C, at various concentrations (7, 15, 31, 61.5, 125, and 250 μM) in cell culture medium containing 10% FCS (fetal calf serum). Following incubation, the samples (450 μl) were centrifuged for 8 min at 11,000 rpm through an ultrafiltration membrane (Amicon Microcon 10 kDa) to separate the bound and free fractions of peptide. Fifty microlitres aliquots of ultrafiltrate were then analyzed by RP-HPLC. Results are expressed as percent free peptide in culture medium.

Anti-viral assay

Cells and HIV virus. Ficoll hypaque-isolated peripheral blood mononuclear cells (PBMCs) were obtained from a healthy donor and PHA-activated for three days. Cells were cultured in RPMI 1640 medium (Roche Products, Mannheim, Germany) supplemented with 20 IU/ml recombinant interleukin-2 (Roche Products), 10% fetal calf serum (FCS, Roche Products), 2 mM L-glutamine (Roche Products), and a 1% penicillin, streptomycin, and neomycin mixture (LifeTechnologies, Grand Island, USA) to a density of 2×10^5 cells/well in a 5% CO_2 atmosphere. Viral stocks (HIV-1_{LAI}) were prepared from PHA-activated umbilical blood mononuclear cell supernatants in the Neurology Service of the Commissariat à l'Energie Atomique (Fontenay aux Roses, France) and kept frozen at −80 °C until use. Fifty percent tissue culture infective dose ($TCID_{50}$) was calculated according to the Kärber formula [12].

Mimetics and control molecules. The PM2, PM3 mimetics, and the CONT1 peptide were diluted in culture medium at concentrations ranging between 200 and 0.5 μM. The anti-CD4 mAb ST40 and the anti-Troponin I mAb 9E8, kindly donated by CNRS UMR 5094, were tested at concentrations ranging between 660 and 6.6 nM. The two other inhibitors, the anti-CD4 mAb Q4120 and Azidothymidine (AZT), were provided by SpiBio (Fontenay aux Roses, France). They were used at concentrations of 0.33–33 and 1–100 nM, respectively.

HIV-1 infection assay. PBMCs (2×10^5/well) were plated in 96-well microplates in culture medium and pre-treated for 1 h at +4 °C with the inhibitors. Pre-treatment with inhibitors was performed in 1% FCS culture medium in the experiment with low $TCID_{50}$ to avoid serum

interference. Cells were then exposed to 100 HIV-1_{LAI} $TCID_{50}$ except for the last experiment, where lower doses of $TCID_{50}$ were used. After incubation for 4 h at 37 °C, each well was washed twice with 100 µl of culture medium. Plates were transferred at 37 °C in a 5% CO_2 atmosphere to allow infection. After 7 days in culture, supernatants were recovered and frozen at −20 °C until use. All experiments were performed in triplicate or quadruplicate. The amount of virus produced by PBMCs was monitored by measuring the reverse transcriptase (RT) activity in the supernatants using RetroSysR RT detection kit (Innovagen, Lund, Sweden). During the experiments, cell viability was microscopically checked by using trypan blue exclusion dye. Neither decrease of the cellular concentration nor presence of cellular fragments or a modification of cellular morphology was observed.

Molecular modeling

Antibody modeling. Molecular modeling of the light and the heavy chain CDRs of the antibody was carried out with the research version of the antibody modeling software A*b*M [10] running on an O2 R5000 Silicon Graphics workstation. The L2, L3, and H1 loops were constructed using canonical Class 1 frameworks and a canonical Class 2 framework for H2, as defined in A*b*M. A new canonical class had to be defined for the unusually long L1 CDR loop of ST40 containing 15 amino acids. Four X-ray structures of antibodies (1ibg, 1mf2, 1acy, and 1ggc) with L1 of 15 residues were identified and superimposed. Each of these L1's had a similar conformation. On the basis of this, the following canonical class for L1 was defined and the X-ray structures missing in the database were added: [TI]-x(20)-C(1)-x(1)-A-x(3)-V-x(7)-S-x(1)-[MLI]-x(1)-W(1)-x(35)-F [10]. The H3 loop of 13 amino acids, which is too long to fit into any H3 classification [13,14], was built using the conformational search program CONGEN [15] implemented in A*b*M, combined with a 3D structural database search. The definition of the building blocks to generate H3 with CONGEN was modified several times to obtain four different models since the 'kinked' feature was not very well defined. The X-ray structure of the antibody 1ibg, containing an L1 and a H3 loop of 15 and 13 residues, was then used to model H3 of ST40 with the same conformation. This model of H3 shows a kink and an extended form. Modeling was achieved through simple mutations and the structure was fully minimized using the Tripos force field. Hydrogens were added to all models of ST40 using the Sybyl software (Tripos) and the models were minimized during 100 iterations with the conjugate gradient method to eliminate all small steric conflicts. The solvent accessible surface areas of ST40 amino acids were calculated on the 3D model of ST40 by the SALVOL program developed by R.S. Pearlman et al. and implemented in Sybyl.

Design of the mimetics and molecular dynamics simulations. All the molecules were visualized and modified using the Sybyl software running on an O2 R5000 Silicon Graphics workstation. For the modeling of the mimetics, CDRs were selected from the antibody, maintained in their original conformations, and then linked together with chemical linkers via appropriate side chains and minimized. Molecular dynamics (MD) simulations of the mimetics were carried out in water with the AMBER force field using the AMBER software (University of California) running on a O200 R10000 Silicon Graphics workstation using four processors. The input files for AMBER were prepared with the XLEAP module. The cross-linking bridge, –CO–NH–, between side chains was defined as an amide bond. The water box was calculated with the module SolvateBox with a box size of 8 Å. The water boxes contained between 2500 and 3500 water molecules for all the simulations and were generated with the WATBOX216 module. This corresponds to a Monte Carlo distribution of water with periodic conditions and constant pressure. The temperature was fixed at 300 K, the cut-off was set at 10 Å, the dielectric constant was set at 1, and the sampling frequency was 1 ps. Before running the dynamics, the solvent molecules were minimized and then the solute. The MD simulations were run for 100 or 300 ps. The first 20 ps of the dynamics were the heating period, during which the system was taken from 10 to 300 K, and it was then increased by 15 K every 1 ps.

Analysis of the MD simulations. The first 50 ps of the MD simulations were not taken into account during the analysis since this was taken as the equilibration time. First, the mimetics at different times during the dynamics simulations were superimposed onto the starting conformer, which was very close to the conformation in the antibody. This displays the deformation of the mimetics during the MD simulation and was carried out using the Sybyl software. The root mean square deviations (RMSDs) were calculated, using the starting conformer as a reference, for each ps of the MD simulation with the CARNAL module from the AMBER package.

Synthesis of mimetics

The syntheses of the mimetics and the control peptide were carried out in a stepwise fashion on an Automated Multiple Peptide Synthesis (AMS 422, ABIMED). HPLC analyses were carried out on a Beckman LC126 system, using Waters SymetryShield column RP18, 5 µm, 100 Å (150 × 4.6 mm) with buffers A: 0.1% TFA in water and B: 0.08% TFA in acetonitrile; gradient from 95% A to 100% B in 12.5 mn with a flow of 1.5 ml/mn. HPLC purifications were carried out on a Waters Prep LC 4000 system, using Waters PrepPak Cartridge C18, 6 µm, 60 Å (40 × 100 mm); gradient from A to 60% B in 60 mn with a flow of 20 ml/mn. Mass analyses were performed using a MALDI-TOF spectrometer (Voyager DE Elite, PE Applied Biosystems) with dihydroxybenzoic acid as matrix. The peptide synthesis was performed using a polyethylene glycol graft polystyrene support (Fmoc-PAL-PEG-PS resin, substitution: 0.41 mmol/g). The Fmoc amino acids were activated in situ by the activating reagents DIPCDI (diisopropylcarbodiimide) and HOBt (1-hydroxybenzotriazole) in DMF (*N*,*N*-dimethylformamide) with a standard fourfold excess. An acetylation step was carried out after each amino acid incorporation to cap possible remaining amine groups and to ensure the absence of deletion peptides. The Fmoc protecting groups were removed by a solution of piperidine in DMF (20%) prior to each coupling. After cleavage of the support and removal of side chain protecting groups by reagent B, a standard TFA-based cocktail (88% TFA, 5% phenol, 5% H_2O, and 4% TIPS [v/v]) and a post-cleavage work-up by ether precipitation were employed. The purity of crude linear peptide was checked by analytical HPLC and mass spectroscopy. If purity was over 85%, the peptide was cyclized at room temperature using 1 equivalent of PyBop and 5 equivalents of $NaHCO_3$ in DMF. The reaction mixture was purified by preparative HPLC and the pure product lyophilized to obtain a white powder with a global yield from 5% to 20%. If purity of the linear peptide was less than 85%, an intermediate purification by preparative HPLC followed by lyophilization was achieved before cyclization. In the case of the mutated mimetic PM2, carrying an isoleucine to lysine substitution, the initial ε-NH_2 function of the lysine was specifically protected by the Alloc (allyloxycarbonyl) protecting group that was removed after the cyclization step according to the following conditions: $Pd[PPh_3]_4$ (3 equivalents), ACN/DMF/AcOH/NMM (7/2/2/1), r.t., 3 H. The pure products were analyzed by analytical HPLC and MALDI-TOF mass spectrometry.

Results and discussion

Modeling of ST40

The amino acid sequence of ST40 and the definition of the CDRs in A*b*M are shown in Fig. 1. ST40 contains two unusually long CDR loops, L1 (15 residues) and H3 (13 residues). The new canonical class identified by us for L1 permitted the construction of this loop in a spe-

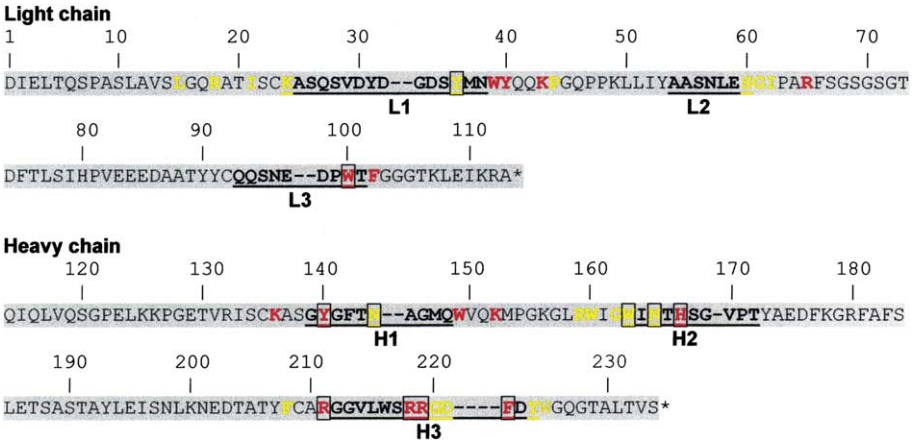

Fig. 1. Amino acid sequence of the variable regions of ST40 antibody. The CDR loops are underlined and bold. The important (red, bold) and less important (orange and yellow, bold) amino acid residues are represented. The residues selected to be included in the mimetic are boxed.

cific conformation, while for the H3 loop several possible conformations were identified. Only four X-ray structures of antibodies containing H3 loops of 13 residues have been described, each having a different conformation. A comparison of the 3D structures of H3 loops containing 11, 12, 13, 14, 15, and 16 residues was carried out and showed that the highest variability occurs at the apex of the loop. However, when the sequence contains an Arg at position N-1 of H3 and Asp-x-Trp at the C-terminus, as in ST40, a kinked form [13,14] is observed at the C-terminal end of the loop. This has been observed in the antibody 1ibg, which contains an L1 and an H3 loop of 15 and 13 residues, respectively. The selected 3D structure of H3 in ST40, containing an extended terminal part of the loop and a kink near the C-terminus, is shown in Fig. 2. This structure was selected as the reference model for the design of ST40 mimetics. However, the inherent flexibility of these longer H3 loops suggested that, during the mimetic construction, care should be taken not to constrain this region of H3 too heavily. Recent advances in the modeling of H3 regions were described by Whitelegg and Rees [16].

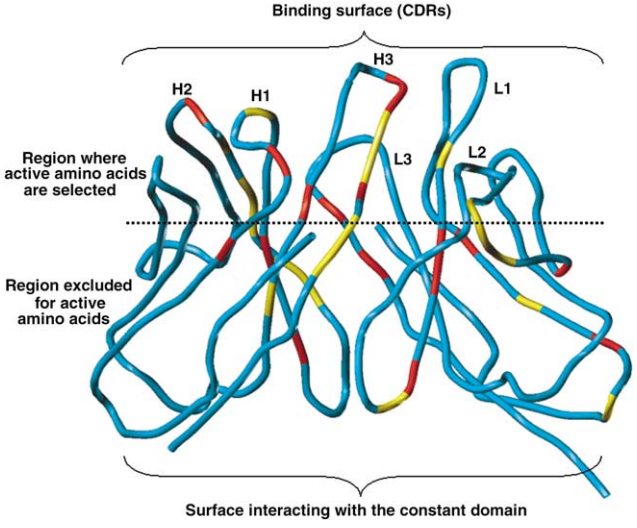

Fig. 2. Ribbon representation of the 3D structure of ST40 and localization of the important (red) and less important (yellow) amino acid residues, as determined by Alanine Scanning. The cut-off for residues with or without accessibility to the antigen is indicated by the dotted line.

Selection of the active chemical groups

The important amino acid residues of ST40, defined by peptide scanning followed by alanine scanning by Monnet et al. [11], are shown in Figs. 1 and 2. It is observed that some important amino acids are not located within, or in some cases even near, the CDR regions where the paratope is located (Fig. 2). To select the amino acids that should be included in the mimetic, the bioactive residues were displayed on the 3D structure of ST40 (Fig. 2) and their accessibility to water was calculated. Some residues were found to be located at some considerable distance from the paratope binding surface (top of Fig. 2), such as Lys152 and Lys43, whereas others were buried in the protein with poor accessibility to antigen. For example, many of the aromatic residues such as Tyr40, Phe102, or Trp149, often playing a structural role in all antibody variable regions, are amongst the buried residues identified as important for antigen binding by the mapping procedure. In contrast, charged residues such as Arg218 and Arg219, more likely to be directly involved in the binding, were conserved. In addition to these hydrophilic residues, amino acids that were predicted to be essential for maintaining the hydrophobic stabilization of the mimetic and which were likely to exhibit increased accessibility in the mimetic because of the flexibility of the H3 loop (e.g., Phe222, Trp163, and Tyr36) were conserved, even though their measured accessibilities on the static

model may have been low. Finally, a limit was fixed for those amino acid residues that should be included in the mimetic based on their importance as defined by the alanine scanning protocol, and their likely accessibility to the antigen. The amino acids selected are boxed in Fig. 1 and displayed on the loops in Fig. 3. All CDRs except L2 are represented in the mimetic by at least one residue. A framework residue located just before the H3 was also included in the mimetic (Arg211). Alanine scanning is a method which might generate false positive "active chemical groups" by exposing residues normally buried in the antibody paratope. As a result, even after careful selection, some of the amino acids selected to be part of the mimetic may not be necessary for binding. However, the first step of this study was to obtain an active mimetic and additional residues should not affect the binding site in the protein. A second step, not targeted in this study, would be the identification of each important residues of the peptide by mutation, to reduce the size of the mimetic. Crystallographic structures of antibody–antigen complexes would provide the optimal starting point for such studies.

Design of cyclic mimetics

To obtain a continuous peptide mimetic amenable to synthesis, the selected amino acids from the CDRs were extracted. The relative locations and orientations in space of the selected amino acid residues, especially the side chains, were conserved and the amino acids were linked together using glycine residues to obtain a cyclic peptide. The cyclization was performed by a covalent bond between the NH_2 of an internal lysine side chain and the C-terminal carboxyl of the peptide. This position was selected to ensure some flexibility within the N terminal segment of the mimetic, which contains the two arginines derived from the flexible H3 loop of ST40. To stabilize the mimetic the glycine residues were then replaced by hydrophobic residues at specific positions, or by proline residues for the turns, to obtain the most stable mimetic in which the important amino acids exhibited similar orientations as observed in the intact parent antibody, ST40. The selection of linking residues was critical for the design. Where possible, residues adjacent to 'active' residues were selected to mimic the environment in the parent antibody and to act in a packing role. For example the Tyr224 was used as a linker for its structural role.

After minimization and short MD simulations (100 ps) of the mimetic, the positions and orientations of the side chains of the important residues were checked. The short MD simulation allows any 'strong' deformation of the mimetic to be observed. At the end of the simulation the conformation of the mimetic was significantly perturbed compared to the starting conformation, and was more energetically favourable. The most stable mimetic from the MD simulations, having the lowest RMSD (4.4 Å) after 100 ps, was selected for synthesis. The amino acid sequence of this mimetic, named PM1, is shown in Table 1 and its starting 3D structure before MD simulation is shown in Fig. 3.

During the first 100 ps of MD simulation of the mimetic PM1, the majority of side chains moved less than 2 Å from their initial positions with the exception of Arg (long side chain) and the aromatic patch containing Phe222, Tyr36, and Trp163 (driven by intra-molecular interactions). After 100 ps, Arg218 and Arg219 within the flexible H3 loop remain oriented at the mimetic surface, pointing outwards into the solvent, as in the starting conformation. The distances between His167 Cβ and Arg219 Cβ, Tyr140 Cβ and Trp163 Cβ, and Asn144 Cβ and Trp100 Cβ are 17, 17, and 18 Å respectively. These are close to those seen in the starting conformation and suggest that global movements within the mimetic maintain the approximately correct distances between critical amino acids from the loops H2–H3, H1–H2, and L3–H1. When the simulation is extended to 300 ps the RMSD increases to 5.49 Å (average of the last 100 ps) due to the inherent flexibility of the peptide. While some deviation of residues from their positions in the original paratope is seen as the simulation progresses, a number of critical residues (His167, Arg218–219, Asn144, and Tyr36) remain in a favorable orientation. Due to problem of interaction of the PM1 mimetic with the sensor ship of the BIAcore, to determine its binding to CD4, the mimetic has to be fixed to the sensor chip using specific functionality. Therefore, a lysine residue was added to the sequence to facilitate the linkage of the mimetic on the sensor chip. Based on the average structure of the final 100 ps of the 300 ps dynamics simulation of PM1, the Ile between Tyr140 and Asn144 was identified as the best location for mutation. At this position the Lys side chain was observed to be pointing away from the surface believed to be important for the CD4 interaction. This change created mimetic PM2 (see Table 1). To demonstrate the importance of the structure of the mimetic for binding to CD4, a non-cyclized mimetic (PM3), having the same sequence as PM2, was synthesized (see Table 1). MD simulations of 300 ps duration were carried out for the peptides PM2 and PM3 using the same starting conformation as for PM1. Surprisingly, the non-cyclized peptide PM3 has a similar 'conformational profile' area as PM2 and maintains also a "compact" structure, probably due to the constraining influence of the five prolines. Indeed, the cyclization of PM1 and PM2 was straightforward during the synthesis. Therefore, as a final control, the peptide CONT1, in which all the linking amino acids of PM3 were mutated to Ala to de-structure the peptide, was synthesized (see Table 1). As expected, during the MD simulation, CONT1 exhibits a completely different conformational distribution—its starting cyclic conformation slowly disappeared during the simulation.

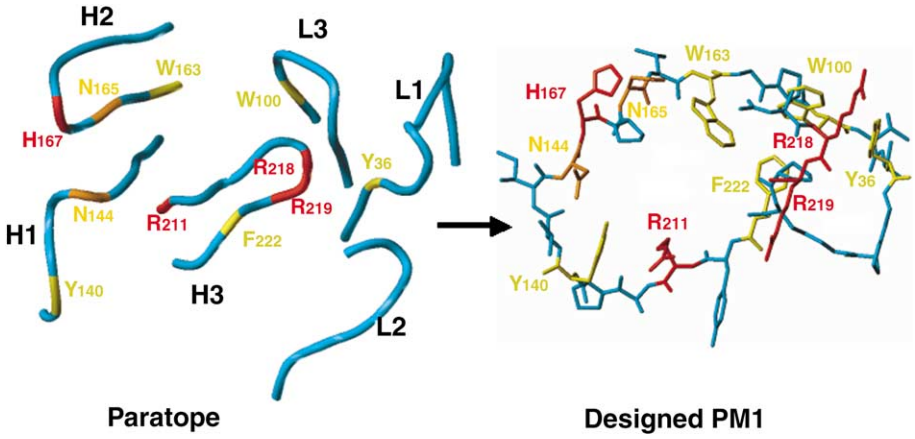

Fig. 3. Representation of the paratope of ST40 and of the resulting mimetic PM1 at 0 ps. The color coding for the important amino acids for inclusion in the mimetic is: red for charged residues (Arg and His), orange for Asn, and yellow for hydrophobic residues (Trp, Phe, and Tyr). The other amino acids of the CDRs are in cyan and the non-CDR residues of the antibody are not shown.

Table 1
Amino acid sequences of the synthesized mimetics

Name	Amino acids sequence
PM1	AcNHA**R**$_{218}$**R**$_{219}$PK**F**$_{222}$Y**R**$_{211}$APY$_{140}$VI**N**$_{144}$**H**$_{167}$P**N**$_{165}$V**W**$_{163}$GP**W**$_{100}$VAY$_{36}$GP—NHCO—
PM2	AcNHA**R**$_{218}$**R**$_{219}$PK**F**$_{222}$Y**R**$_{211}$APY$_{140}$VK**N**$_{144}$**H**$_{167}$P**N**$_{165}$V**W**$_{163}$GP**W**$_{100}$VAY$_{36}$GP—NHCO—
PM3	AcNHA**R**$_{218}$**R**$_{219}$PK**F**$_{222}$Y**R**$_{211}$APY$_{140}$VK**N**$_{144}$**H**$_{167}$P**N**$_{165}$V**W**$_{163}$GP**W**$_{100}$VAY$_{36}$GP**COOH**
CONT1	AcNHA**R**$_{218}$**R**$_{219}$AA**F**$_{222}$A**R**$_{211}$AAY$_{140}$AK**N**$_{144}$**H**$_{167}$A**N**$_{165}$A**W**$_{163}$AA**W**$_{100}$AAY$_{36}$AA**COOH**

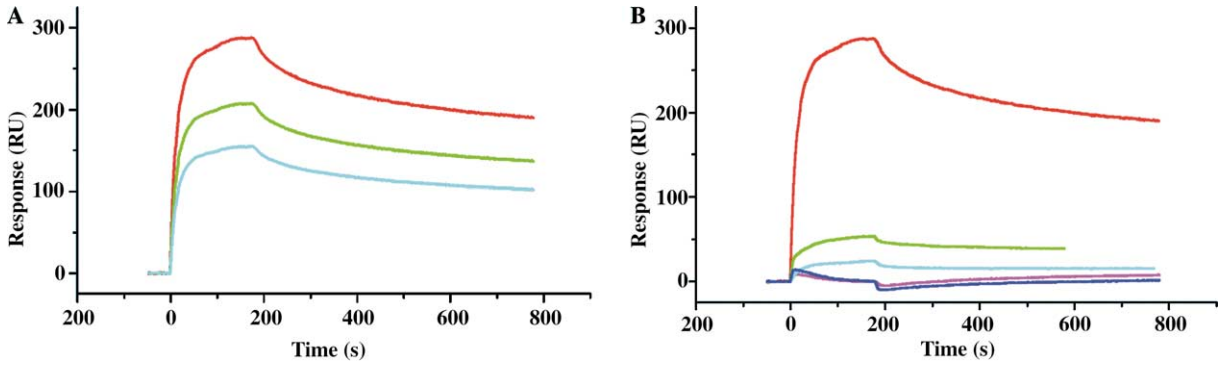

Fig. 4. (A) Sensorgrams of CD4 (50 nM, light blue; 99 nM, green; and 198 nM, red) binding to peptide PM2 immobilized on the sensor chip. (B) Sensorgrams of binding competition by injection of pre-incubated CD4 + ST40 (green) and CD4 only (red) when the mimetic PM2 is immobilized on the sensor chip. The binding of CD4 on CONT1 (blue) and to the irrelevant proteins 2C2 (pink) and TnC (dark blue) to PM2 is also represented.

BIAcore analysis

BIAcore sensorgrams for the binding of soluble CD4 to immobilized mimetic PM2 are shown in Fig. 4A. Kinetic constants were measured and gave values of $k_a = 10.4 \times 10^5\ M^{-1}\ s^{-1}$ and $k_d = 0.94 \times 10^{-4}\ s^{-1}$. The calculated K_D was 0.9 nM. The interaction of three irrelevant proteins (2C2, an anti-digoxin Mab, Troponin

C, and albumin) with the immobilized mimetic was also tested and the results are shown in Fig. 4B. No binding was observed for control proteins, except with albumin, which interacts with many peptides. For the competition study, ST40 mAb (660 nM, 50 μg/ml) and CD4 (165 nM, 20 μg/ml) were pre-mixed, and then co-injected on the sensor chip (Fig. 4B). The subsequent binding of CD4 to the mimetic was inhibited by 70%. This demonstrated that the mimetic PM2 binds to the same, or very closely located, site on CD4 as the parent antibody, ST40. A competition assay, with the CD4 fixed on the sensor ship and the peptide and ST40 co-injected, would have been more appropriate to demonstrate the binding competition, but the stickiness of the mimetic to the sensor ship did not permit us to perform this experiment.

The binding of PM3 to CD4 was not perturbed by the absence of covalent cyclization and its kinetic parameters were similar to those of PM2 (graphical data not shown) ($k_a = 9.03 \times 10^4\,M^{-1}\,s^{-1}$ and $k_d = 1.69 \times 10^{-4}\,s^{-1}$) with a calculated K_D of 1.87 nM. As for PM2, no irrelevant protein binding was observed, while pre-incubation of CD4 with ST40 inhibited 80% of CD4 binding to PM3 (Fig. 4B). As expected, the peptide CONT1 showed no binding to CD4 (Fig. 4B). These experimental results are entirely consistent with the MD simulation analysis of the PM2, PM3, and CONT1.

The affinities of PM2 and PM3, 0.9 and 1.9 nM, respectively, compared to 0.37 nM for the antibody [11], are very promising results for an antibody mimetic and lift these molecules into the range required for in vivo therapeutic activity.

Anti-retroviral activity assays

The ability of the anti-CD4 mimetics to inhibit viral reverse transcriptase activity was measured in PBMCs infected with 100 HIV-1_{LAI} $TCID_{50}$.

Protein binding of the peptides PM2, PM3, and CONT1 was measured using a 10% SVF culture medium (identical to that used in the cellular assays). After ultrafiltration using Microcon filters, 16 μM of PM2, for example, was found in the ultrafiltrate for an initial concentration of 125 μM. When all the results were averaged, the measured protein binding for the three compounds was: 85% of PM2, 82% of PM3, and 89% of CONT1. The observed non-specific 'stickiness' in a solution of PM2 and PM3, possibly originates from the hydrophobic 'underbelly' of the construct.

In the viral assay, the non-specific antibody 9E8 mAb showed no inhibitory activity, in contrast to AZT and Q4120 mAb, which inhibited RT activity in a dose-dependent manner (Table 2). Culturing PBMCs with the PM2 mimetic prior to infection with HIV led to the inhibition of viral reverse transcription, as also demonstrated for the parental anti-CD4 mAb ST40. The inhibitory activity was dose-dependent, with an IC_{50} for PM2 of ~7 μM (after correction for non-protein bound mimetic). The IC_{50} of the parental mAb was ~20 nM. Neither the negative control antibody 9E8 nor the CONT1 mimetic showed any dose-dependent activity, as expected. Higher concentration of PM2 was not tested due to problem of precipitation of the peptide in the presence of serum.

Table 2
Inhibition of viral particle production by anti-CD4 mimetic PM2

Inhibitor	Concentration	Inhibition of RT activity (%) first series	Inhibition of RT activity (%) second series
AZT	100 nM	100 ± 0	100 ± 0
	10 nM	74 ± 13	72 ± 17
	1 nM	66 ± 5	17 ± 17
9E8 mAb	660 nM	−5 ± 8	
	66 nM	13 ± 29	
	6.6 nM	−12 ± 11	
Q4120 mAb	33 nM	96 ± 0	
	3.3 nM	56 ± 16	
	0.33 nM	8 ± 11	
ST40 mAb	660 nM	96 ± 0	
	66 nM	83 ± 3	
	6.6 nM	14 ± 11	
PM2 mimetic	100 μM		98 ± 3
	50 μM	51 ± 13	74 ± 34
	5 μM	23 ± 5	—
	0.5 μM	−3 ± 6	—
CONT1	50 μM		11 ± 35
	10 μM		22 ± 25
	5 μM		−7 ± 30

Viral production was followed by measuring RT activity in cell-free supernatant. PBMCs were pre-treated with various inhibitors, washed, and then exposed to 100 $TCID_{50}$ of HIV_{LAI}. The data have been calculated from three triplicate experiments (means ± SD).

Finally, in order to assess the ability of the PM2 mimetic to reduce the viral titer, as the control Q4120 antibody does, we measured RT activity after infection of PBMCs with low HIV-1_{LAI} doses, ranging between 16 and 0.8 $TCID_{50}$. No viral replication was observed in the four culture wells tested, corresponding to PBMCs pre-treated with 100 μM (15 μM of free mimetic) PM2 and infected with 8 $TCID_{50}$, whereas 11 out of 12 culture wells infected with 8 $TCID_{50}$, but not pre-treated with PM2, showed viral replication. No cell death was seen during any of the assays (data not shown).

The low HIV cellular inhibition activity of PM2 was surprising considering high binding to CD4. Should cross-linking, or other ancillary effects on CD4 molecules by ST40, and other neutralizing antibodies, be advantageous for preventing HIV infection, this might explain the lower activity despite an essentially identical affinity for CD4. Again, the cellular assay took place over a period of 7 days so that the high stability of an intact antibody in the cellular milieu compared with a

smaller peptide would be likely to affect the overall activity performance.

Conclusions

We have described here a new approach, which is still under development and by which many different antibodies, whose function may simply be blocking of a pharmacologically relevant protein surface interaction, might be replaced by a smaller molecule. When applied to therapeutically important antibodies, the smaller size, easier production, and lower cost of the synthetic mimetics may offer significant advantages compared to recombinant antibodies or antibody fragments. This process seems promising given the binding interaction obtained, but needs to be reproduced in several antibody/antigen interaction systems, including those where binding alone is the functional readout. Such an approach obviously would not be appropriate where the full antibody structure plays a role in stabilising the antigen.

Acknowledgments

We acknowledge Mr. P. Turi and Dr. C. Quétard (BIACORE, France) for their useful advice and assistance for some of the BIAcore assays. We thank Steve Searle and Nicholas Whitelegg for help with aspects of the antibody modeling. We also acknowledge the French Research Minister for financial support.

References

[1] C.O. Ogbu, M.N. Qabar, P.D. Boatman, J. Urban, J.P. Meara, M.D. Ferguson, J. Tulinsky, C. Lum, S. Babu, M.A. Blaskovich, H. Nakanishi, F. Ruan, B. Cao, R. Minarik, T. Little, S. Nelson, M. Nguyen, A. Gall, M. Kahn, Highly efficient and versatile synthesis of libraries of constrained beta-strand mimetics, Bioorg. Med. Chem. Lett. 8 (1998) 2321–2326.

[2] B.-W. Park, H.-T. Zhang, C. Wu, A. Berezov, X. Zhang, R. Dua, Q. Wang, G. Kao, D.M. O'Rourke, M.I. Greene, R. Murali, Rationally designed anti-HER2/neu peptide mimetic disables $P185^{HER2/neu}$ tyrosine kinase in vitro and in vivo, Nature Biotech. 18 (2000) 194–198.

[3] G. Tuchscherer, B. Dörner, B. Sila, B. Kamber, M. Mutter, The TASP concept: mimetics of peptide ligands, protein surfaces and folding units, Tetrahedron 49 (1993) 3559–3575.

[4] M. Mutter, S. Vuilleumier, A chemical approach to protein design-template-assembled synthetic proteins (TASP), Angew. Chem. Int. Ed. Engl. 28 (1989) 535–554.

[5] C. Vita, J. Vizzavona, E. Drakopoulou, S. Zinn-justin, B. Gilquin, A. Ménez, Novel miniproteins engineered by the transfer of active sites to small natural scaffolds, Biopolymers 47 (1998) 93–100.

[6] R. Li, V. Dowd, D.J. Stewart, S.J. Burton, C.R. Lowe, Design, synthesis, and application of a protein A mimetic, Nature Biotech. 16 (1998) 190–195.

[7] U. Reineke, R. Sabat, R. Misselwitz, H. Welfle, H.D. Volk, J. Schneider-Mergener, A synthetic mimic of a discontinous binding site on interleukin-10, Nature Biotech. 17 (1999) 271–275.

[8] F. Falcioni, K. Ito, D. Vidovic, C. Belunis, R. Cambell, S.J. Berthel, D.R. Bolin, P.B. Gillespie, N. Huby, G.L. Olson, R. Sarabu, J.-M. Guenot, V. Madison, J. Hammer, F. Sinigaglia, M. Steinmetz, Z.A. Nagy, Peptidomimetic compounds that inhibit antigen presentation by auto immune disease-associated class II major histocompatibility molecules, Nature Biotech. 17 (1999) 562–567.

[9] D. Laune, F. Molina, G. Ferrieres, J.-C. Mani, P. Cohen, D. Simon, T. Bernardi, M. Piechaczyk, B. Pau, C. Granier, Systematic exploration of the antigen binding activity of synthetic peptides isolated from the variable regions of immunoglobulins, J. Biol. Chem. 272 (1999) 30937–30944.

[10] S. Searle, J. Pedersen, A. Henry, D.M. Webster, A.R. Rees, Antibody structure and function, in: C.A.K. Borrebaeck (Ed.), Antibody Engineering, Oxford University Press, New York, 1995, pp. 13–51.

[11] C. Monnet, D. Laune, J. Laroche-Traineau, M. Biard-Piechaczyk, L. Briant, C. Bes, M. Pugniere, J.-C. Mani, B. Pau, M. Cerutti, G. Devauchelle, C. Devaux, C. Granier, T. Chardes, Synthetic peptides derived from variable regions of an anti-CD4 monoclonal antibody bind to CD4 and inhibit HIV-1 promoter activation in virus-infected cells, J. Biol. Chem. 274 (1999) 3789–3796.

[12] G. Kärber, Arch. Exp. Path. Pharmak. 162 (1931) 956–959.

[13] H. Shirai, A. Kidera, H. Nakamura, Structural classification of CDR-H3 in antibodies, FEBS Lett. 399 (1996) 1–8.

[14] H. Shirai, N. Nakajima, H. Higo, A. Kidera, H. Nakamura, Conformational sampling of CDR-H3 in antibodies by multicanonical molecular dynamics simulation, J. Mol. Biol. 278 (1998) 481–496.

[15] R.E. Bruccoleri, M. Karplus, Prediction of the folding of short polypeptide segments by uniform conformational sampling, Biopolymers 26 (1987) 137–168.

[16] N.R. Whitelegg, A.R. Rees, WAM: an improved algorithm for modelling antibodies on the WEB, Protein Eng. 13 (2000) 819–824.